Available online at www.sciencedirect.com
ScienceDirect
Journal of Solid State Chemistry 179 (2006) 3974–3980
JOURNAL OF SOLID STATE CHEMISTRY
www.elsevier.com/locate/jssc

Monoclinic phase of the misfit-layered cobalt oxide $(Ca_{0.85}OH)_{1.16}CoO_2$

Mitsuyuki Shizuya, Masaaki Isobe*, Yuji Baba, Takuro Nagai, Yoshio Matsui, Eiji Takayama-Muromachi

National Institute for Materials Science (NIMS), 1-1 Namiki, Tsukuba, Ibaraki 305-0044, Japan

Received 9 June 2006; received in revised form 7 September 2006; accepted 12 September 2006
Available online 17 September 2006

Abstract

A monoclinic phase of the misfit-layered cobalt oxide $(Ca_{0.85}OH)_{1.16}CoO_2$ was successfully synthesized and characterized. It was found that this new material is a poly-type phase of the orthorhombic form of $(CaOH)_{1.14}CoO_2$, recently discovered by the present authors. Both the compounds consist of two interpenetrating subsystems: CdI_2-type CoO_2 layers and rock-salt-type double-atomic-layer CaOH blocks. However, these two phases exhibit a different stacking structure. By powder X-ray and electron diffraction (ED) studies, it was found that the two subsystems of $(Ca_{0.85}OH)_{1.16}CoO_2$ have *c*-centered monoclinic Bravais lattices with common $a = 4.898$ Å, $c = 8.810$ Å and $\beta = 95.8°$ lattice parameters, and different *b* parameters: $b_1 = 2.820$ Å and $b_2 = 4.870$ Å. Chemical analyses revealed that the monoclinic phase has a cobalt valence of $+3.1$–3.2. Resistivity of the monoclinic phase is approximately 10^1–10^5 times lower than that of the orthorhombic phase. This suggests that the monoclinic phase is a hole-doped phase of the insulating orthorhombic phase. Furthermore, large positive Seebeck coefficients ($\sim$100 μV/K) were observed near room temperature.

Keywords: Layered cobalt oxide; Misfit-layered compound; Thermoelectric oxide; High-pressure synthesis; New-material design; Electron microscopy

1. Introduction

Layered cobalt oxides have attracted much attention because the compounds are an electrically and magnetically intriguing low-dimensional system. The compounds exhibit the ability to generate large thermoelectric power in spite of relatively high electrical conductivity [1]. Thus, they have been studied in terms of the generation mechanism of thermoelectric power, ultimately to find new materials that possess high thermoelectric properties for energy conversion. Furthermore, recently discovered unconventional superconductivity in $Na_{0.35}CoO_2 \cdot 1.3H_2O$ has stimulated researchers to further study these compounds [2].

The layered cobalt oxides have common crystal structure features. The crystal structure consists of CdI_2-type conducting CoO_2 layers and insulating blocking layers. Accordingly, if we replace the blocking layer with any other type of structure while keeping the CoO_2 layer, we can obtain a new class of materials. This idea resembles the guiding principle for new-material design of the homologous series of high-T_C cuprate superconductors. The layered cobalt oxides can be classified by the number of atomic layers *n* in the blocking layer. In the case of $n = 1$, the blocking layer consists of a single atomic layer such as $Na_{0.7}CoO_2$ [1]. In the case of $n \geqslant 2$, the blocking layer consists of multiple atomic layers of a rock-salt-type crystal structure. The corresponding compounds are rich in variety, e.g., $[Sr_2O_2]_{0.5}CoO_2$ ($n = 2$) [3], $[Ca_2CoO_3]_{0.62}CoO_2$ ($n = 3$) [4,5], $[Ca_2(Co_{0.65}Cu_{0.35})_2O_4]_{0.63}CoO_2$ ($n = 4$) [6], and $[Bi_{0.87}SrO_2]_2[CoO_2]_{1.82}$ ($n = 4$) [7]. Most of these compounds have lattice incommensurability between the rock-salt-type block and the CoO_2 layer, yielding structural modulation due to lattice mismatch. The compounds are therefore so-called "misfit-layered compounds".

Recently, we have discovered and reported a new misfit-layered cobalt oxide $(CaOH)_{1.14}CoO_2$ prepared using the high-pressure synthesis technique [8]. This compound is the first material of the $n = 2$ member, and belongs to the class of composite crystals. The basic crystal structure is the orthorhombic form, which includes the rock-salt-type

*Corresponding author. Fax: +81 29 860 4674.
E-mail address: ISOBE.Masaaki@nims.go.jp (M. Isobe).

0022-4596/$ - see front matter © 2006 Elsevier Inc. All rights reserved.
doi:10.1016/j.jssc.2006.09.008

CaOH double atomic layers alternatively stacking with the CoO_2 layers. The most distinctive feature of this compound is that the blocking layer does not contain any valence-changeable ions, such as transition-metal elements. Accordingly, it means that this compound is the most suitable phase for the observation of the electronic states in the CoO_2 layer. The actual cobalt valence of the orthorhombic $(CaOH)_{1.14}CoO_2$ is about $+3$, so the compound can be regarded as a parent material of the system. Following the new-phase search of the compound, our next purpose was to look at carrier doping in the $(CaOH)_{1.14}CoO_2$ phase, thinking that it may possibly lead to an improvement of the thermoelectric power or to the discovery of a higher T_C superconductor. Actually, by controlling the composition of the materials, we recently succeeded in synthesizing a compound that is another $n = 2$ member of the hole-doped Ca–Co–O–H system.

In this paper, we report on the synthesis method, crystal structure, chemical compositions, and electrical resistivity data of the new cobalt calcium hydroxide $(Ca_{0.85}OH)_{1.16}CoO_2$. X-ray and electron diffraction (ED) studies revealed that this compound exhibits a *c*-centered monoclinic lattices structure and is a poly-type phase of the orthorhombic form $(CaOH)_{1.14}CoO_2$. These phases consist of the same sub-lattice blocks, but the stacking of the blocks is different in each phase. The monoclinic $(Ca_{0.85}OH)_{1.16}CoO_2$ has a higher cobalt valence of about $+3.1$–3.2 and is more conductive than the orthorhombic $(CaOH)_{1.14}CoO_2$ because of the hole doping. By the chemical analysis, we found that the carrier source of the hole doping is due to the calcium deficiency. Our studies revealed that the present phase is structurally similar to the $Ca_{25}Co_{22}O_{56}(OH)_{28}$ phase recently reported by Klimczuk et al. [9]. However, the chemical composition and the cobalt valence is quite different from that reported.

2. Experiment

Two polycrystalline samples were prepared from a solid-state reaction, employing a high-pressure synthesis technique, using the mixtures Co_3O_4 (99.9%), CaO_2 (99%), CaO, and $Ca(OH)_2$ [10]. The starting reagents with appropriate atomic molar ratios of Ca:Co:O:H = 1:1:3.333:1.167 (sample-A) and = 1:1:3.333:1.417 (sample-B) were mixed in an agate mortal in a glove box filled with dry Ar gas. Each mixture was then encapsulated in a gold tube. The two capsules were simultaneously heated in a flat-belt-type high-pressure apparatus under 6 GPa at 1200 °C for 1 h, then quenched to room temperature before releasing the pressure. The as-grown products were individually pulverized and washed in deionized water to remove the small amount of unreacted $Ca(OH)_2$ phase.

The crystal structure was studied using powder X-ray diffraction (XRD) and transmission electron microscopy. The XRD data were collected using a Bragg-Brentano type diffractometer (Rigaku, RINT2200HF-ULTIMA) with a CuK_α radiation source. Lattice constants were determined from the least-squares method using fundamental Bragg reflections for each subsystem. Electron diffraction (ED) images were taken using a microscope (Hitachi H-1500) operating at 820 kV. The powder sample was dispersed in CCl_4 using an ultrasonic cleaner. The supernatant fluid containing fine powder was collected and dropped onto carbon micro-grids for observation.

Cation ratios of the high-pressure phase in the sample were determined from an electron-probe microanalysis (EPMA) using a wavelength-dispersive X-ray spectrometer (JEOL JXA-8500F) with an acceleration voltage of 15 kV. In EPMA, a small ceramic specimen of the unwashed bulk sample was well polished using a 0.3 μm alumina lapping film to obtain a flat surface. Several relatively large grains were selected and analyzed. The average grain size of the phase was about $50 \times 20\,\mu m^2$.

After dissolving the sample powder in hydrochloric acid, the amount of cobalt atoms in a specimen was determined using inductively coupled plasma atomic emission spectrometry (ICP-AES). The oxidation state of the cobalt ion was determined from redox titration. The washed powder sample was dissolved in sulfuric acid containing an excess of sodium oxalate $(COONa)_2$, as a reducing agent. The residual $(COONa)_2$ was titrated against an aqueous solution of potassium permanganate ($KMnO_4$) to reduce the oxidation state of the cobalt ions.

Hydrogen in the sample was determined from an infrared (IR) absorption spectroscopic analysis with a carbon/hydrogen analyzer (LECO RC-412). During the measurement, as temperature increased, hydrogen atoms in the sample reacted with oxygen atoms in the phase and/or carrier oxygen gas, and simultaneously yielded H_2O vapor. Intensity of the IR-absorption spectrum due to the vaporized H_2O was recorded during heating. The amount of H_2O in the sample was determined by calibrating the intensity data using a standard material; $Na_2WO_4 \cdot 2H_2O$. To avoid detecting the water adhering onto grain surfaces and/or boundaries, the samples were pre-heated at 150 °C before measurement.

Electrical resistivity of the unwashed bulk sample was measured from the conventional four-probe alternating current (AC) method using a commercial apparatus (Quantum Design, PPMS). The sample size was $1.3 \times 2.0 \times 5.5\,mm^3$. The distance between the voltage terminals was 2.4 mm. Copper wires were attached onto the polished sample surface via an evaporated gold film using silver paste in order to make a good ohmic contact. An AC current of 0.5–0.01 mA at 60–300 Hz was applied to the sample for the measurement.

Seebeck coefficients were measured from the PPMS using a thermal transport option (TTO) with a four probe configuration. Data were collected through a continuous mode while cooling at 0.3 K/min. Temperatures at the two temperature/voltage terminals were measured using thermometers (Cernox 1050). The temperature difference between the two terminals was controlled to within 3% of the measurement temperature.

3. Results and discussion

Fig. 1 is the powder XRD patterns of sample-A and the orthorhombic $(CaOH)_{1.14}CoO_2$. The former phase is the subject material in the present work, while the latter is another new phase that we recently reported in Ref. [8]. The two XRD patterns look similar; for sample-A, three peaks corresponding to the $0\,0\,l\,0$ ($l = 1$, 2 or 3) lines are observed in the low-angle range of 2-θ ($2\theta < 35^\circ$). However, these lines are at a lower 2-θ angle than the corresponding peaks of the orthorhombic phase, indicating that the interlayer distance in the present phase is somewhat longer than that in the orthorhombic phase. In addition, the XRD patterns of the small peaks observed in the high-angle range ($2\theta > 35^\circ$) are significantly different from each other. This indicates that the present phase is not identical to the orthorhombic phase.

In Fig. 1(b), all the diffraction peaks including the small reflections can be systematically indexed using sets of four integers, $h\,k\,l\,m$, by assuming that the present phase is a composite crystal having a (3 + 1)-dimensional structure with two c-centered monoclinic subsystems with common a, c and β, and two different b parameters. The XRD data are listed in Table 1. The lattice parameters of samples-A and B are summarized in Table 2. The lattice parameters of each subsystem were calculated using the fundamental reflections of the $m = 0$ indices for the first subsystem and the $k = 0$ indices for the second subsystem. The b_1, b_2 and a parameters of the monoclinic $(Ca_{0.85}OH)_{1.16}CoO_2$ are nearly equal to the a_1, a_2 and b parameters of the orthorhombic $(CaOH)_{1.14}CoO_2$, respectively. The $c \times \sin(\beta)$ of the monoclinic phase is approximately half of c of the orthorhombic phase [8]. This indicates that the crystal structure of the present compound is similar (but not identical) to that of the orthorhombic $(CaOH)_{1.14}CoO_2$.

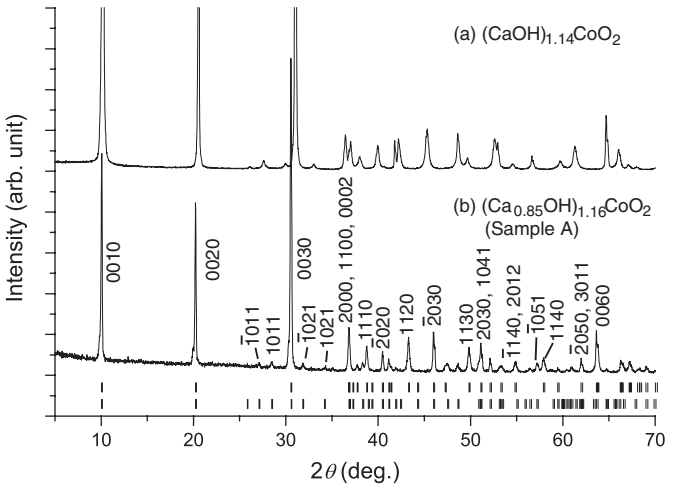

Fig. 1. Powder X-ray diffraction patterns of two poly-type phases of the new misfit-layered cobalt oxides: (a) orthorhombic $(CaOH)_{1.14}CoO_2$ [8] and (b) monoclinic $(Ca_{0.85}OH)_{1.16}CoO_2$ (sample-A). The short vertical bars indicate fundamental-reflection positions for the two subsystems of the monoclinic phase; the upper-bars and the lower-bars correspond to subsystem-1 (CoO_2) and subsystem-2 ($Ca_{0.85}OH$), respectively.

Figs. 2(a)–(c) are the ED images of the sample-A projected along the [001], [100] and [0−1 0] directions, respectively. Fig. 2(a) is a typical ED pattern on a^*–b^* section, most frequently observed because the crystal easily cleaves along the a–b plane. This image is essentially identical to that observed in the orthorhombic $(CaOH)_{1.14}CoO_2$ [8]. A hexagonal-like reciprocal unit lattice due to the CoO_2 block and a tetragonal-like reciprocal unit lattice due to the CaOH block are clearly observed in the image. This indicates that the present phase is a composite crystal consisting of the two subsystems.

In Fig. 2, fundamental reciprocal-lattice vectors of the two subsystems are highlighted by arrows. The angle between the $\boldsymbol{a}^*$- and $\boldsymbol{c}^*$-axis is approximately 84.6° ($= 180^\circ - \beta$). The other crystallographic angles, α and γ, are 90°. This clearly indicates that the Bravais lattice of the present phase is monoclinic. All of the diffraction spots, both the main and satellite reflections, can be assigned using a linear combination of the four unit vectors, $\boldsymbol{a}^*$, $\boldsymbol{b}_1^*$, $\boldsymbol{c}^*$, $\boldsymbol{b}_2^*$, and four integers, $h\,k\,l\,m$, with the reciprocal-lattice vector, $\boldsymbol{q}$ ($d = 1/|\boldsymbol{q}|$), given by the following equation: $\boldsymbol{q} = h\boldsymbol{a}^* + k\boldsymbol{b}_1^* + l\boldsymbol{c}^* + m\boldsymbol{b}_2^*$. The $|\boldsymbol{b}_2^*|/|\boldsymbol{b}_1^*|$ obtained is approximately 0.58, consistent with the b_1/b_2 ($= 0.5791(2)$) value obtained from the XRD study. Reflection conditions for the fundamental spots are $h + k = 2n$ ($hk00$), $k = 2n$ ($0kl0$) and $h = 2n$ ($h0l0$) for subsystem-1, and $h + m = 2n$ ($h00\,m$), $m = 2n$ ($00lm$) and $h = 2n$ ($h0l0$) for subsystem-2, which indicates that each subsystem has a c-centered lattice. Therefore, possible space groups of the fundamental structures for the two subsystems are, $C2/m$ (No. 12), Cm (No. 8) and $C2$ (No. 5).

Projections of a possible crystal structure model for the present monoclinic phase along the [010] and the [−1 0 0] directions are illustrated in Figs. 3(b) and (c), respectively. The highest-symmetry space group $C2/m$ of the three possible space groups was employed to describe the structure. The structural model of the orthorhombic phase is illustrated in Fig. 3(a) for comparison. It is found that the two phases exhibit similar compositions; i.e., $(CaOH)_{1.14}CoO_2$ for the orthorhombic phase and $(Ca_{0.85}OH)_{1.16}CoO_2$ for the monoclinic phase. In contrast, however, the compounds exhibit different unit cells. The difference between the two phases is the stacking of the CoO_2 and CaOH blocks along the c-axis. The orthorhombic phase is composed of an A–B–A'–B' stacking sequence, whereas the monoclinic phase is A–B–A–B stacking; the stacking sequence in each case is periodic (see Figs. 3(a) and (b)). This structural difference is known as "polytypism". A similar polytypism has been observed in the layered sulfide $(PbS)_{1.18}TiS_2$ [11].

Table 3 lists results of the chemical analysis and the interlayer distances of the monoclinic $(Ca_{0.85}OH)_{1.16}CoO_2$ and orthorhombic $(CaOH)_{1.14}CoO_2$. The monoclinic phase could be synthesized from the starting composition of $CaCoO_{3.333}H_{1.167}$ (sample-A) and $CaCoO_{3.333}H_{1.417}$

Table 1
Powder X-ray diffraction data of the monoclinic $(Ca_{0.85}OH)_{1.16}CoO_2$ (sample-A, CuK_α radiation)

$2\theta_{obs.}$ (deg)	$2\theta_{cal.}$ (deg)		h	k	l	m	I/I_0 (%)
	Subsystem-1	Subsystem-2					
10.059	10.082	10.082	0	0	1	0	56.1
20.217	20.243	20.244	0	0	2	0	47.3
27.113		27.109	−1	0	1	1	1.5
28.512		28.480	1	0	1	1	1.6
30.539	30.568	30.569	0	0	3	0	100.0
31.828		31.854	−1	0	2	1	2.0
34.195		34.201	1	0	2	1	1.2
36.838	36.853	36.854	2	0	0	0	13.2
37.735	37.722		−1	1	1	0	1.8
38.314		38.333	0	0	1	2	2.4
38.757	38.756		1	1	1	0	7.6
40.474	40.469	40.472	−2	0	2	0	6.4
41.139	41.155	41.156	0	0	4	0	4.4
41.361	41.388		−1	1	2	0	1.6
41.901		41.903	1	0	3	1	1.4
43.261	43.289		1	1	2	0	10.7
45.983	45.995	45.999	−2	0	3	0	14.2
47.241	47.263		−1	1	3	0	2.1
47.482		47.527	−1	0	4	1	2.7
48.642		48.633	0	0	3	2	2.1
49.837	49.826		1	1	3	0	7.6
50.824		50.905	1	0	4	1	2.9
51.120	51.121	51.119	2	0	3	0	9.6
52.118	52.124	52.125	0	0	5	0	5.3
53.123		53.128	2	0	0	2	1.6
53.320	53.288	53.292	−2	0	4	0	1.6
54.820	54.822		−1	1	4	0	3.3
56.402		56.442	0	0	4	2	1.3
57.182		57.191	−1	0	5	1	3.2
57.901	57.898		1	1	4	0	4.6
59.438	59.442	59.440	2	0	4	0	2.0
60.396		60.361	−2	0	3	2	1.2
60.940		60.919	1	0	5	1	1.9
61.980	61.966	61.972	−2	0	5	0	5.1
63.639	63.635	63.636	0	0	6	0	15.5
64.715		64.736	1	0	2	3	1.7
66.281	66.264		−3	1	1	0	4.6
67.256	67.240		1	1	5	0	3.8
68.159	68.102		−3	1	2	0	1.4
68.394	68.346		3	1	1	0	1.4
69.021	69.007	69.004	2	0	5	0	2.6
70.067	70.035		0	2	2	0	0.6
71.863	71.862	71.868	−2	0	6	0	3.5
73.822	73.832		−1	1	6	0	3.4
75.935	75.916	75.918	0	0	7	0	2.4
77.202	77.222		−3	1	4	0	0.9
77.762	77.764		3	1	3	0	1.2
78.503	78.514		−2	2	1	0	1.7
78.503		78.496	0	0	0	4	1.7
79.783	79.792	79.789	2	0	6	0	4.3

(sample-B), while the orthorhombic phase was obtained from the starting composition of $Ca_{1.117}CoO_{3.14}H_{1.049}$ [8]. It suggests that excess oxygen, excess hydrogen and/or calcium deficiency in the starting composition are necessary for crystallization of the monoclinic phase for synthesis. The actual compositions determined by the chemical analysis indicate that the monoclinic phase includes approximately 15% deficit in the calcium atoms as compared with the ideal composition of $(CaOH)_{1.16}CoO_2$. In addition, the experimental results suggest that there are excess hydrogen and oxygen atoms in the phase. Possibly, the excess hydrogen atoms or oxonium ions (H_3O^+) may partly compensate for the defects of the calcium site. However, the calcium deficiency seems to be consistent

Table 2
Lattice parameters of the monoclinic samples-A and B, and the orthorhombic sample prepared from the different starting compositions

Starting composition	Crystallographic system	Subsystem	a (Å)	b (Å)	c (Å)	β (deg)	b_1/b_2
$CaCoO_{3.333}H_{1.167}$	Monoclinic	1: $[CoO_2]$	4.8987(7)	2.8202(5)	8.8109(7)	95.772(8)	0.5791(2)
(sample-A)		2: [CaOH]	4.8985(9)	4.8700(7)	8.8106(7)	95.766(9)	
$CaCoO_{3.333}H_{1.417}$	Monoclinic	1: $[CoO_2]$	4.9008(7)	2.8217(4)	8.7735(9)	95.82(1)	0.5785(2)
(sample-B)		2: [CaOH]	4.8993(6)	4.877(1)	8.7765(5)	95.831(7)	
			b (Å)	a (Å)	c (Å)		a_1/a_2
$Ca_{1.117}CoO_{3.14}H_{1.049}$[a]	Orthorhombic	1: $[CoO_2]$	4.9228(4)	2.8238(2)	17.275(1)	90	0.5711(4)
		2: [CaOH]	4.9228(4)	4.944(2)	17.275(1)	90	

[a]Cited from Ref. [8].

with the fact that the lattice parameters of the CaOH sub-lattice, a and b_2, of the monoclinic phase are approximately 0.5% and 1.4% smaller than those of the orthorhombic phase (calcium-deficiency-free phase).

The actual cobalt valence of the monoclinic phase is about +3.1–3.2. This value is larger than that of the orthorhombic phase (+2.9–3.0) and is rather close to those of other layered cobalt oxides exhibiting CoO_2 layers [12]. This suggests that the hole carriers are doped into the cobalt t_{2g} band for the monoclinic phase. We found that the interlayer distance between the CoO_2 layers, d, increases with respect to increases in the cobalt valence. This is probably due to changes of charge balance between the sub-lattices. The hole doping into the Co atoms reduces net charges in the CoO_2 block, which tends to neutralize coulombic attraction between the CoO_2 block and the rock-salt-type one, resulting in the interlayer-distance expansion.

Recently, Klimczuk et al. [9] have reported a similar phase of the Ca–Co–O–H system ($Ca_{25}Co_{22}O_{56}(OH)_{28}$). The lattice parameters, the structure, and the symmetry of the phase are almost equal to those of the phase reported in this paper. However, the cobalt valence that Klimczuk et al. report (+4.0) is quite different from the result obtained in this study (+3.1–3.2). We have never succeeded in synthesizing such a high-valence Ca–Co–O–H system. Unfortunately, no direct evidence for such a high cobalt valence is reported in the authors' paper. From a comparison between the interlayer distance ($c \times \sin(\beta) = 8.78$ Å) reported by Klimczuk et al. and the current d values in Table 3, we suppose that the correct cobalt valence of the Klimczuk et al. phase is about 3.1–3.2, and thus, this phase is the same material as the phase reported in this paper.

Fig. 4 is the plot of the resistivity as a function of temperature for the monoclinic $(Ca_{0.85}OH)_{1.16}CoO_2$ (sample-A). The resistivity data of the orthorhombic $(CaOH)_{1.14}CoO_2$ are also plotted in the figure as a comparison [8]. The absolute values of the resistivity in the monoclinic phase are about 10^{-1}–$10^{2}\,\Omega$ cm, which is about 10^{1}–10^{5} times lower in magnitude than those of the orthorhombic phase. This agrees well with the fact that holes are doped into the phase. However, the resistivity values of the monoclinic phase are still somewhat larger than those of other layered cobalt oxides such as $[Ca_2CoO_3]_{0.62}CoO_2$ [4,13], The resistivity-gradient of the monoclinic phase still remains semiconductor-like ($d\rho/dT<0$). We suppose that this is principally due to slightly insufficient carrier doping in the phase. In addition, the calcium deficiency may also affect the carrier conduction through enhancement of the potential randomness for the phase.

It is worth noting that the resistivity of the monoclinic phase abruptly increases with decreasing temperature below ~25 K. This looks to be anomalous behavior, probably due to carrier localization. We found that in this temperature range the T-dependence of the resistivity can be well approximated using the equation, $\rho = \rho_0 \exp(T_0/T)^{1/2}$, often observed in compounds dominated by the Efros and Shklovskii type variable-range hopping regime (ES-VRH) [14]. Inset of Fig. 4 is the $\ln(\rho)$ vs. $1/T^{1/2}$ plot, and clearly indicates that the plot is a straight line for $T \leqslant 25$ K ($1/T^{1/2} \geqslant 0.2$). The origin of this T-dependence is not clear at present. However, the ES-VRH type regime may be the mechanism of conduction for the present phase.

Fig. 5 is the Seebeck coefficients S of the monoclinic $(Ca_{0.85}OH)_{1.16}CoO_2$. The positive sign of S indicates that the carrier type is a hole. The absolute value at room temperature (~100 μV/K) is about one-third of that of the orthorhombic sample (~330 μV/K) and is as large as the S values of the other typical layered cobalt oxides such as Na_xCoO_2 [1] and $Ca_3Co_4O_9$ [4]. The behavior of the T-dependence of S above 6.5 K is also similar to that of the other cobalt oxides: the S increases with temperature and eventually saturates near room temperature.

It should be noted that the Seebeck coefficient abruptly increases with decreasing temperature below 6.5 K. This anomalous divergence of S may be related to the enhancement of resistivity observed at low temperatures. This behavior in S can be explained by assuming that a band-gap is produced at the Fermi level. However, we found that the observed data in the low-temperature range cannot be well approximated using the simple formula for conventional band-gap semiconductors: $S = (k_B/e)(A + E_g/2k_BT)$ (A is the temperature independent term, E_g the gap energy). In contrast, it is theoretically expected that the Seebeck coefficient does not depend on temperature in the

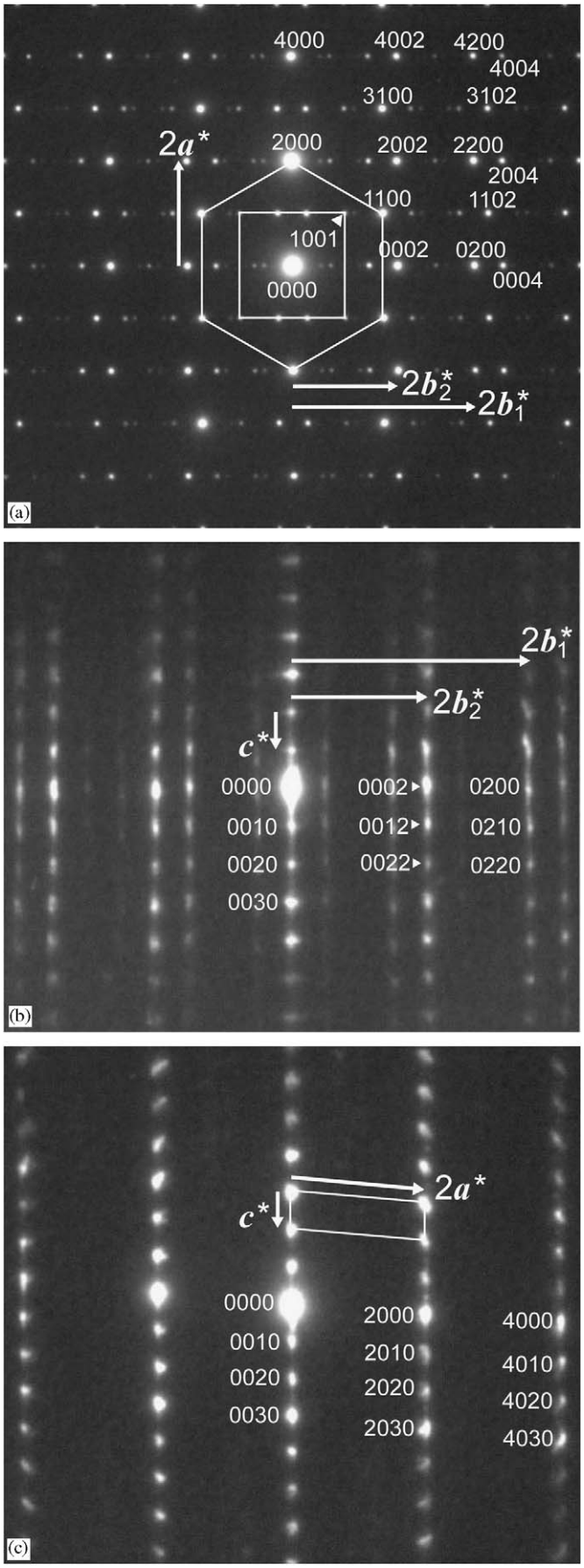

case of the ES-VRH type carrier conduction [15,16]. The observed experimental fact contradicts both the existing simple theories. We presume that a more complicated electronic state may exist in the present monoclinic phase $(Ca_{0.85}OH)_{1.16}CoO_2$. To understand the reason for the anomalous behavior in the carrier conduction and the thermoelectric-power at low temperature, further experiments and precise analyses are required.

In summary, we successfully synthesized a new misfit-layered cobalt oxide $(Ca_{0.85}OH)_{1.16}CoO_2$. This compound has monoclinic symmetry and is a poly-type phase of the orthorhombic $(CaOH)_{1.14}CoO_2$ [8]. Crystal structures of these phases exhibit different stacking of the two subsystems: the CdI_2-type CoO_2 block (subsystem-1) and the rock-salt-type CaOH block (subsystem-2). We studied the crystal structure of specimens using X-ray and ED and found that all diffraction peaks (and spots) can be systematically indexed using four integers, $hklm$, with the reciprocal-lattice vectors $\boldsymbol{q}$, from the formula, $\boldsymbol{q} = h\boldsymbol{a}^* + k\boldsymbol{b}_1{}^* + l\boldsymbol{c}^* + m\boldsymbol{b}_2{}^*$; the lattice parameters in real space are $a = 4.898$ Å, $b_1 = 2.820$ Å, $b_2 = 4.870$ Å, $c = 8.810$ Å and $\beta = 95.8^\circ$. Chemical analyses revealed that the phase partly contains a calcium deficiency in the rock-salt-type blocks, and the cobalt valence is about +3.1–3.2. This indicates that the monoclinic phase is the hole-doped phase of the orthorhombic. Absolute values of the resistivity of the monoclinic phase are 10^{-1}–$10^{2}\,\Omega$ cm, markedly lower than those of the orthorhombic phase. However, the temperature-dependence behavior of the resistivity still remains semiconductor-like. In particular,

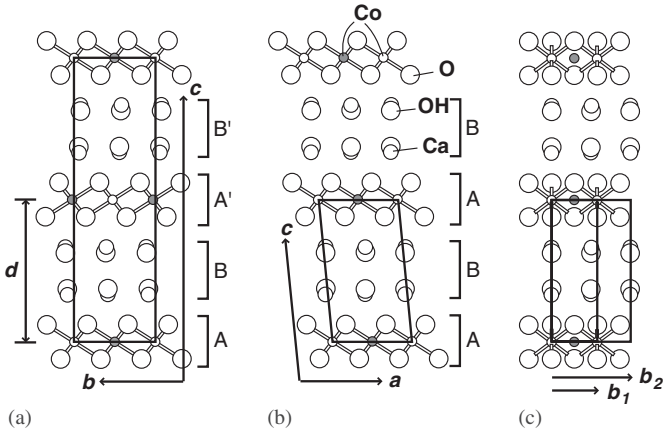

Fig. 3. Projections of the crystal structure of the poly-type phases of $(Ca_{1-\delta}OH)_xCoO_2$. Large circles are oxygen atoms or hydroxyl groups, middle-size circles are calcium atoms, small circles are cobalt atoms, and the white and gray-coloring represents 1/2 difference along each projection axis. d is the interlayer distance between the CoO_2 layers. (a) Projection along the a-axis of the orthorhombic structure. (b) Projection along the b-axis of the monoclinic structure. (c) Projection along the [−100] direction of the monoclinic structure. In each case, the rectangle is the unit cell.

Fig. 2. Electron diffraction (ED) patterns projected along the (a) [001], (b) [100], and (c) [0−10] directions for the monoclinic $(Ca_{0.85}OH)_{1.16}CoO_2$ (sample-A).

Table 3
Chemical analysis results of the two monoclinic samples-A and B, and the orthorhombic sample

Starting composition	Co-valence[a]	Ca/Co[b]	H_2O wt%[c]	Chemical composition[d]	d (Å)[e]
$CaCoO_{3.333}H_{1.167}$ (sample-A)	3.16 ± 0.04	0.985 ± 0.007	8.0 ± 0.8 (7.43, 8.57)	$(Ca_{0.849\pm0.006}O_{1.07\pm0.09}H_{1.2\pm0.1})_{1.16}CoO_2$	8.766(8)
$CaCoO_{3.333}H_{1.417}$ (sample-B)	3.08 ± 0.04	1.00 ± 0.01	8.8 ± 0.5 (8.41, 9.11)	$(Ca_{0.862\pm0.009}O_{1.12\pm0.07}H_{1.28\pm0.09})_{1.16}CoO_2$	8.728(9)
$Ca_{1.117}CoO_{3.14}H_{1.049}$[f]	2.94 ± 0.04	1.14 ± 0.02	6.9 ± 0.14(7.0, 6.8)	$(Ca_{1.00\pm0.02}O_{1.06\pm0.05}H_{1.05\pm0.04})_{1.14}CoO_2$	8.6375(5)

[a]Measured using redox titration and ICP measurement. Error bars were estimated from the magnitude of the experimental errors and sensitivity of the detection device.
[b]Measured using EPMA. Error bars are the standard deviation of original data detected at five grains in a ceramic sample.
[c]Measured using the IR absorption method. Error bars are the standard deviation of original data obtained from two powder samples (in the parentheses).
[d]Calculated from the measured values of Ca/Co, Co-valence and H_2O wt%.
[e]Interlayer distance between the CoO_2 layers.
[f]Cited from Ref. [8].

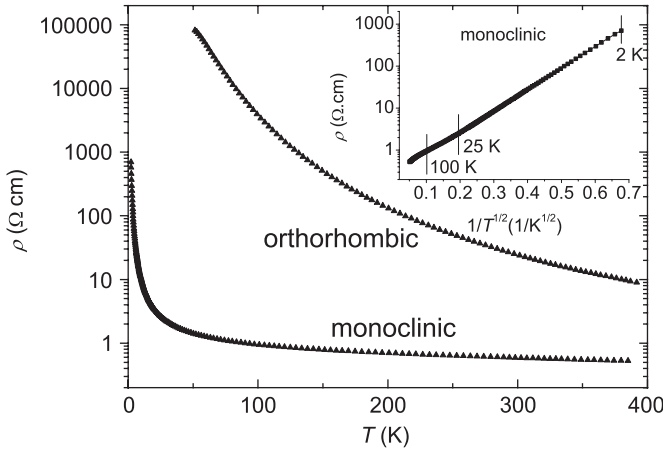

Fig. 4. Resistivity as a function of temperature for the monoclinic $(Ca_{0.85}OH)_{1.16}CoO_2$ (sample-A) and orthorhombic $(CaOH)_{1.14}CoO_2$ [8]. Inset indicates the Efros–Shklovskii-type variable-range-hopping plot ($\ln(\rho)$ vs. $1/T^{1/2}$) of the resistivity data for the monoclinic phase.

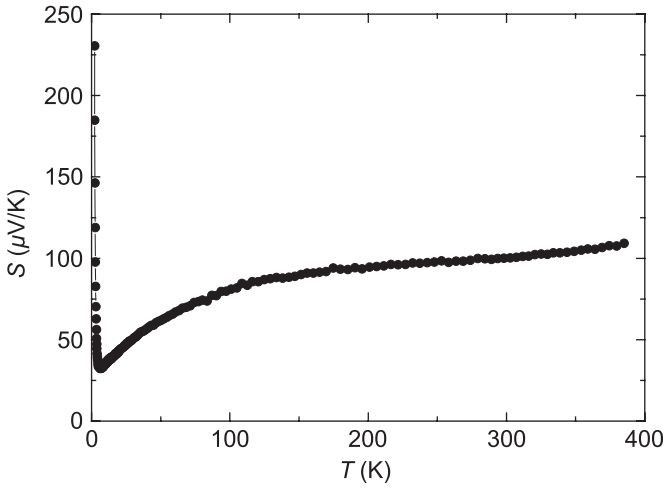

Fig. 5. The Seebeck coefficient as a function of temperature for the monoclinic $(Ca_{0.85}OH)_{1.16}CoO_2$ (sample-A).

we found anomalous strong carrier localization below ~25 K, suggesting that there is a Coulomb gap approximately at the Fermi energy. The Seebeck coefficient shows the typical temperature dependence as a layered cobalt oxide above 6.5 K and exhibits the large absolute value around room temperature.

Acknowledgment

We thank S. Takenouchi of NIMS for ICP-AES and redox titration, and K. Kosuda of NIMS for EPMA. We also express sincere thanks to Dr. Taniguchi for a lot of helpful advice on the high-pressure experiments. This research was partly supported by the Superconducting Materials Research Project administrated by the Ministry of Education, Culture, Sports, Science and Technology of Japan.

References

[1] I. Terasaki, Y. Sasago, K. Uchinokura, Phys. Rev. B 56 (1997) R12685.
[2] K. Takada, H. Sakurai, E. Takayama-Muromachi, F. Izumi, R.A. Dilanian, T. Sasaki, Nature 422 (2003) 53.
[3] H. Yamauchi, K. Sakai, T. Nagai, Y. Matsui, M. Karppinen, Chem. Mater. 18 (2006) 155.
[4] A.C. Masset, C. Michel, A. Maignan, M. Hervieu, O. Toulemonde, F. Studer, B. Raveau, J. Hejtmanek, Phys. Rev. B 62 (2000) 166.
[5] Y. Miyazaki, M. Onoda, T. Oku, M. Kikuchi, Y. Ishii, Y. Ono, Y. Morii, T. Kajitani, J. Phys. Soc. Jpn. 71 (2002) 491.
[6] Y. Miyazaki, T. Miura, Y. Ono, T. Kajitani, Jpn. J. Appl. Phys. 41 (2002) L849.
[7] H. Leligny, D. Grebille, O. Pérez, A.C. Masset, M. Hervieu, B. Raveau, Acta Crystallogr. B 56 (2000) 173.
[8] M. Shizuya, M. Isobe, Y. Baba, T. Nagai, M. Osada, K. Kosuda, S. Takenouchi, Y. Matsui, E. Takayama-Muromachi, J. Solid State Chem., submitted for publication, cond-mat/0510031.
[9] T. Klimczuk, H.W. Zandbergen, N.M. van der Pers, L. Viciu, V.L. Miller, M.-H. Lee, R.J. Cava, cond-mat/0510137 (2005).
[10] The CaO was prepared by heating $CaCO_3$ (99.9%) at 1100 °C for a day in flowing dry Ar gas. The $Ca(OH)_2$ was prepared from the CaO powder by reaction with ion-exchanged water. The reacted $Ca(OH)_2$ powder was dried at 300 °C in Ar gas before use.
[11] S. van Smaalen, J.L. de Boer, Phys. Rev. B 46 (1992) 2750.
[12] Y. Morita, J. Poulsen, K. Sakai, T. Motohashi, T. Fujii, I. Terasaki, H. Yamauchi, M. Karppinen, J. Solid State Chem. 177 (2004) 3149.
[13] Y. Miyazaki, K. Kudo, M. Akoshima, Y. Ono, Y. Koike, T. Kajitani, Jpn. J. Appl. Phys. 39 (2000) L531.
[14] A.L. Efros, B.I. Shklovskii, J. Phys. C 8 (1975) L49.
[15] I.P. Zvyagin, in: M. Pollak, B. Shklovskii (Eds.), Hopping Transport in Solids, Elsevier, North-Holland, Amsterdam, 1991, p. 143.
[16] N.V. Lien, D.D. Toi, Phys. Lett. A 261 (1999) 108.